

VISUAL GROUPING BY NEURAL OSCILLATORS

Guoshen Yu

CMAP, Ecole Polytechnique,
91128 Palaiseau Cedex, France

Jean-Jacques Slotine

NSL, Massachusetts Institute of Technology
Cambridge, MA 02139, USA

ABSTRACT

Distributed synchronization is known to occur at several scales in the brain, and has been suggested as playing a key functional role in perceptual grouping. State-of-the-art visual grouping algorithms, however, seem to give comparatively little attention to neural synchronization analogies. Based on the framework of concurrent synchronization of dynamic systems, simple networks of neural oscillators coupled with diffusive connections are proposed to solve visual grouping problems. The same algorithm is shown to achieve promising results on several classical visual grouping problems, including point clustering, contour integration and image segmentation.

Index Terms— visual grouping, neural oscillator, synchronization, segmentation, clustering.

1. INTRODUCTION

Consider Fig. 1. Why do we perceive in these visual stimuli a cluster of points, a straight contour and a hurricane? How is the identification performed between a subgroup of stimuli and the perceived objects?

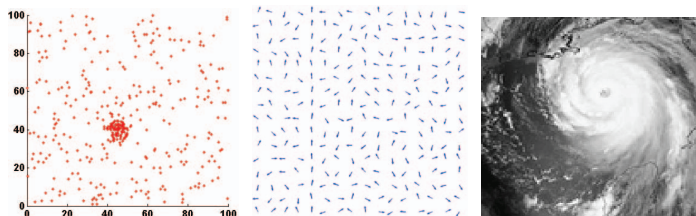


Fig. 1. Left: a cloud of points in which a dense cluster is embedded. Middle: a random direction grid in which a vertical contour is embedded. Right: an image in which a hurricane is embedded.

Many physiological studies, e.g. [5], have shown evidence of grouping in visual cortex. Gestalt psychology [9], an attempt to formalize the laws of visual perception, addresses some grouping principles such as proximity, good continuation and color constancy, in order to describe the construction of larger groups from atomic local information in the stimuli.

In the brain, at a finer level of functional detail, the distributed *synchronization* known to occur at different scales has been proposed as a general functional mechanism for perceptual grouping [1, 13, 16]. In computer vision, however, comparatively little attention has been devoted to exploiting neural-like oscillators in visual grouping (see [3, 12] for example). Wang and his colleagues have performed very innovative work

using oscillators for image segmentation [2]. They constructed oscillator networks with local excitatory lateral connections and a global inhibitory connection. Yen and Finkel [17] simulated facilitatory and inhibitory interactions among oscillators to do contour integration. Li has proposed elaborate visual cortex models with oscillators [8] and applied them on lattice drawings. Kuzmina and his colleagues [7] have constructed a simple self-organized oscillator coupling model, and applied it on synthetic lattice images as well. Faugeras et al. have started studying oscillatory neural mass models in the contexts of natural and machine vision [4].

In this paper we propose a simple and general neural oscillator algorithm for visual grouping, based on diffusive connections [11]. We use full-state neural oscillator models rather than phase-based approximations. The key to our approach is to embed the desired grouping properties in the *couplings* between oscillators. This allows one to exploit existing results on visual grouping and Gestalt while at the same time taking advantage of the flexibility and robustness afforded by synchronization mechanisms. Synchronization of oscillators induces perceptual grouping while desynchronization leads to segregation. Applications to point clustering, contour integration, and segmentation of synthetic and real images are demonstrated. A recent study of stable concurrent synchronization of neural oscillators [11] provides a general analysis tool to model the associated nonlinear dynamics and study their convergence properties.

Section 2 introduces a basic model of neural oscillators with diffusive coupling connections and proposes a general visual grouping algorithm. Sections 3, 4 and 5 describe in detail the neural oscillator solutions for point clustering, contour integration and image segmentation and show a number of examples. The results are compared with normalized cuts, a popular computer vision method [3, 12]. Section 6 presents brief concluding remarks.

2. MODEL AND ALGORITHM

The model is a network of neural oscillators coupled with diffusive connections. Each oscillator is associated to an atomic element in the stimulus, such as a point, an orientation or a pixel. Without coupling, the oscillators are desynchronized and oscillate in random phases. Under diffusive coupling with the coupling strength appropriately tuned, they may converge to multiple groups of synchronized elements. The synchronization of oscillators within each group indicates that perceptual grouping of the underlying stimulative atoms, while the desynchronization between groups suggests group segregation.

2.1. Neural Oscillators

We use a modified form of FitzHugh-Nagumo neural oscillators [6, 10], similar to [2],

$$\dot{v}_i = 3v_i - v_i^3 - v_i^7 + 2 - w_i + I_i \quad (1)$$

$$\dot{w}_i = c[\alpha(1 + \tanh(\beta v_i)) - w_i] \quad (2)$$

where v_i is the membrane potential of the oscillator, w_i is an internal state variable representing gate voltage, I_i represents the external current input, and α , β and c are strictly positive constants (we use $\alpha = 12$; $c = 0.04$; $\beta = 4$). When the input I_i exceeds a certain threshold value, the neural oscillator oscillates, the trace of membrane potential v_i being plotted in Fig. 2-a. Other spiking oscillator models can be used similarly. In the neural oscillator networks for visual grouping, each oscillator is associated to an atomic element in the stimuli.

2.2. Diffusive connections

Oscillators are coupled using diffusive connections with Gaussian-tuned gains to form networks.

Let us denote by $\mathbf{x}_i = [v_i, w_i]^T$ the state vectors of the oscillators introduced in section 2.1, each with dynamics $\dot{\mathbf{x}}_i = \mathbf{f}(\mathbf{x}_i, t)$. A neural oscillator network is composed of N oscillators, connected with diffusive coupling [15]

$$\dot{\mathbf{x}}_i = \mathbf{f}(\mathbf{x}_i, t) + \sum_{i \neq j} k_{ij}(\mathbf{x}_j - \mathbf{x}_i), \quad i = 1, \dots, N \quad (3)$$

where k_{ij} is the coupling strength.

Oscillators i and j are said to be synchronized if \mathbf{x}_i remains equal to \mathbf{x}_j . Once the elements are synchronized, the coupling terms disappear, so that each individual element exhibits its natural, uncoupled behavior, as illustrated in Fig. 2. It is intuitive to see that a larger k_{ij} value facilitates and reinforces the synchronization between the oscillators i and j (refer to [11, 15] for more details).

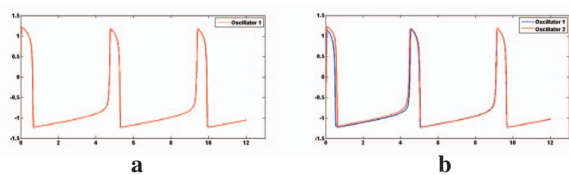


Fig. 2. **a.** a single oscillator. **b.** synchronization of two oscillators coupled through diffusive connections. The two oscillators start to be fully synchronized at about $t = 5$.

The key to applying neural oscillators with diffusive connections to visual grouping is to tune the coupling so that the oscillators synchronize if their underlying atoms belong to the same visual group, and desynchronize otherwise. According to Gestalt psychology [9], visual stimulus atoms of similarity or proximity tend to be grouped perceptually. This suggests that the coupling between the neural oscillators should be reinforced if they have similar stimuli. Such coupling can be implemented by the Gaussian tuning

$$k_{ij} = e^{\frac{-|s_i - s_j|^2}{\beta^2}}. \quad (4)$$

where s_i and s_j are stimuli of the two oscillators, for example position for point clustering, orientation for contour integration and grey-level for image segmentation, and β is a tuning parameter.

2.3. Concurrent Synchronization and Stability

In perception, fully synchronized elements in each group are bounded, while different groups are segregated. Concurrent synchronization analysis provides a mathematical tool to study stability and exponential convergence properties in this context.

In an ensemble of dynamical elements, concurrent synchronization is defined as a regime where the whole system is divided into multiple groups of fully synchronized elements, but elements from different groups are not necessarily synchronized [11]. Networks of oscillators coupled by diffusive connections are specific cases of this general framework. It can be shown that with appropriate coupling gains, the networks converge to concurrent synchronization with high convergence rates. The reader is referred to [11] for more details on the analysis tools.

2.4. Visual Grouping Algorithm

The basic visual grouping algorithm proceeds in the following steps.

1. Construct a neural oscillator network. Each oscillator is associated to one atom in the stimuli. Oscillators are connected with diffusive connections (3) using the Gaussian-tuned gains (4).
2. The oscillators converge to concurrently synchronized groups in the so-constructed network.
3. Identify the synchronized oscillators and equivalently the visual groups. A group of synchronized oscillators indicates that the underlying visual stimulative atoms are perceptually grouped. Desynchronization between groups suggests that the underlying stimulative atoms in the two groups are segregated.

Traces of synchronized oscillators coincide in time, while those of desynchronized groups are separated [14]. The identification of synchronization in the oscillation traces (as illustrated in the example of Fig. 3-b) can be realized by thresholding the correlation of the traces [17] or by simply applying a clustering algorithm such as k -means.

3. POINTS CLUSTERING

Let us denote $\mathbf{y}_i = (x_i, y_i)$ the coordinates of a point \mathbf{p}_i . Each point \mathbf{p}_i is associated to an oscillator \mathbf{x}_i . The proximity gestalt principle [9] suggests strong coupling between oscillators corresponding to proximate points. More precisely, the coupling strength between \mathbf{x}_i and \mathbf{x}_j is

$$k_{ij} = \begin{cases} e^{\frac{-|\mathbf{y}_i - \mathbf{y}_j|^2}{\beta^2}} & \text{if } j \in \mathcal{N}_i \\ 0 & \text{otherwise} \end{cases}, \quad (5)$$

where \mathcal{N}_i is a neighborhood of \mathbf{p}_i . For example \mathcal{N}_i can be defined as the set of M points closest to \mathbf{p}_i . Then (5) couples an oscillator \mathbf{x}_i with its M nearest neighbors. The local coupling can propagate to make the coupling in a larger scale. Higher M value reinforces the coupling. The parameter β tunes the size of the clusters one expects to detect. The external inputs I_i of the oscillators in (1) are set as uniformly distributed random variables in the appropriate range.

Fig. 3 illustrates an example in which the points clearly make two clusters. As shown in Fig. 3-b, the oscillator system converges to two concurrently synchronized groups, each corresponding to one cluster, and separated in the time dimension. The identification of the two groups induces the clustering of the underlying points, as shown in Fig. 3-c.

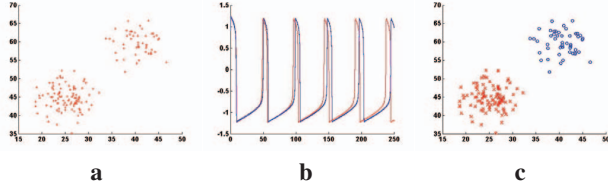


Fig. 3. **a.** Points to cluster. **b.** The oscillators converge to two concurrently synchronized groups. **c.** Clustering results. The blue circles and the red crosses represent the two clusters.

Fig. 4 presents a more challenging setting where one seeks to identify a cluster in a cloud of points. The cloud is made of 300 points uniformly randomly distributed in a space of size 100×100 , in addition to a cluster of 100 Gaussian distributed points with standard deviation equal to 3×3 . Thanks to the coupling (5), the neural oscillator system converges to one synchronized group that corresponds to the cluster with all the “outliers” totally desynchronized in the background, as shown in Fig. 4-b. The synchronized traces are segregated from the background by thresholding the correlation among the traces (threshold = 0.99) [17] which results in the identification of the underlying cluster, as shown in Fig. 4-c. The result of normalized cuts [12] is illustrated in Fig. 4-d: a large number of outliers are confused to the cluster of interest.

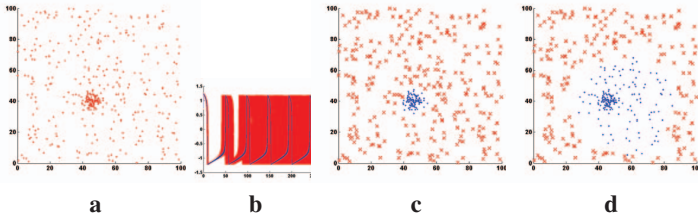


Fig. 4. **a.** A cloud of points made of 300 points uniformly randomly distributed in a space of size 100×100 , in addition to a cluster of 100 Gaussian distributed points with standard deviation equal to 3×3 . **b.** The neural oscillator system converges to one synchronized group that corresponds to the cluster with all the “outliers” totally desynchronized in the background. **c.** and **d.** Clustering results by respectively neural oscillators and normalized cuts: blue dots represent the cluster detected by the algorithm and red crosses are the “outliers”. In the latter many outliers are confused to the cluster of interest.

4. CONTOUR INTEGRATION

Fig. 5 shows the setting of the contour integration experiments. An orientation value $\mathbf{o}_i \in [0, 2\pi)$ is defined for each element $\mathbf{i} = (i, j)$ in a grid as illustrated by the arrows. Each orientation in the grid is associated to one oscillator. The coupling of the oscillators \mathbf{i} and \mathbf{j} follows the Gestalt law of “good continuation” and, in particular, the results of the psychovisual experiments of Field et al [5]:

$$k_{ij} = \begin{cases} \exp\left(-\frac{|\mathbf{o}_i - \mathbf{o}_j|^2}{\delta^2} - \frac{|\frac{\mathbf{o}_i + \mathbf{o}_j}{2} - \mathbf{o}_{ij}|^2}{\gamma^2}\right) & \text{if } \|\mathbf{i} - \mathbf{j}\| \leq w \\ 0 & \text{otherwise} \end{cases} \quad (6)$$

where

$$\mathbf{o}_{ij} = \begin{cases} \arctan(\mathbf{i} - \mathbf{j}) & \text{if } \left| \arctan(\mathbf{i} - \mathbf{j}) - \frac{|\mathbf{o}_i + \mathbf{o}_j|}{2} \right| \\ < \left| \arctan(\mathbf{i} - \mathbf{j}) + \pi - \frac{|\mathbf{o}_i + \mathbf{o}_j|}{2} \right| \\ \arctan(\mathbf{i} - \mathbf{j}) + \pi & \text{otherwise} \end{cases}$$

is the unidirectional orientation of the path \mathbf{ij} (the closer to the average element-to-element orientation $\frac{|\mathbf{o}_i + \mathbf{o}_j|}{2}$ modulo π). By making smoothness constraints on the element-to-element angle (the first term in (6)) and the element-to-path angle (the second term in (6)), the neural oscillator system provides smooth contour integration, with δ and γ tuning the smoothness of the detected contour. Contour integration is known to be rather local [5], and the coupling (6) is effective within a neighborhood of size $(2w + 1) \times (2w + 1)$. In the experiments the parameters are chosen as $\delta = 20^\circ$, $\gamma = 10^\circ$ and $w = 1$, in line with the results of the psychovisual experiments of Field et al [5].

Fig. 5-a shows a grid in which orientations are uniformly distributed in space, except for one vertical contour. The orientation of the elements on the vertical contour undertakes furthermore a Gaussian perturbation of standard deviation $\sigma = 10^\circ$. The neural oscillator system converges to one synchronized group that corresponds to the contour with all the other oscillators desynchronized (the traces are similar to Fig. 4-b). As in [17], the synchronized group is segregated by thresholding the correlation among the traces (threshold = 0.99). This results in the “pop-out” of the contour shown in Fig. 5-b. As shown Fig. 5-c, the multiscale normalized cut [3] does not succeed in segregating the contour from the background. Fig. 6 illustrates a similar example with two intersected straight contours.

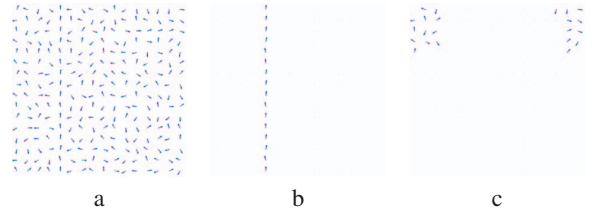


Fig. 5. **a.** A vertical contour is embedded in a uniformly distributed orientation grid. **b.** and **c.** Contour integration by respectively neural oscillators and normalized cuts.

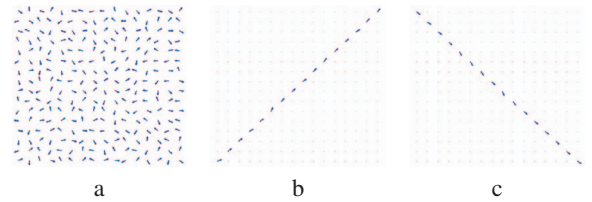


Fig. 6. **a.** Two contours embedded in a uniformly distributed orientation grid. **b.** and **c.** the two contours identified by neural oscillators.

Fig. 7-a illustrates a smooth curve embedded in the uniformly randomly distributed orientation background. With some minor effort, subjects are able to identify the curve due to its “good continuation”. Similarly the neural system segregates the curve from the background with the oscillators lying on the curve fully synchronized, as illustrated in Fig. 7-b.

5. IMAGE SEGMENTATION

One oscillator is associated to each pixel in the image. Within a neighborhood the oscillators are non-locally coupled with a coupling strength

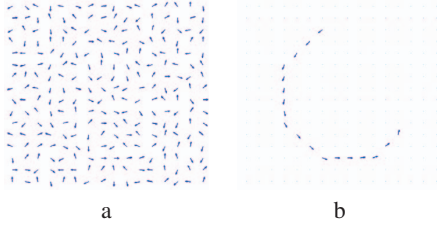


Fig. 7. **a.** A smooth curve is embedded in a uniformly distributed orientation grid. **b.** The curve detected by neural oscillators.

$$k_{ij} = \begin{cases} e^{-\frac{|u_i - u_j|^2}{\beta^2}} & \text{if } |\mathbf{i} - \mathbf{j}| < w \\ 0 & \text{otherwise} \end{cases} \quad (7)$$

where u_i is the pixel gray-level at coordinates $\mathbf{i} = (i, j)$ and w adjusts the size of the neighborhood. Pixels with similar grey-levels are coupled more tightly, as suggested by the color constancy gestalt law [9]. Non-local coupling plays an important role in regularizing the image segmentation, with a larger w resulting in more regularized segmentation and higher robustness to noise.

Fig. 8-a illustrates a synthetic image (the gray-levels of the black, gray and white parts are 0, 128, and 255) contaminated by white Gaussian noise of moderate standard deviation $\sigma = 10$. The segmentation algorithm was configured with $\beta = \sigma$ and $w = 5$. The oscillators converge into three concurrently synchronized groups as plotted in Fig. 8-b which results in a perfect segmentation as shown in Fig. 8-c.

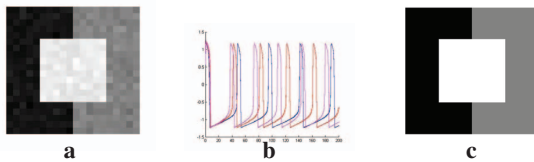


Fig. 8. **a.** A synthetic image (the gray-levels of the black, gray and white parts are respectively 0, 128, 255) contaminated by white Gaussian noise of standard deviation $\sigma = 10$. **b.** The traces of the neural oscillation. The oscillators converge into three concurrently synchronized groups. **c.** Segmentation result.

Fig. 9 show some natural image segmentation examples in comparison with the multiscale normalized cuts [3]. Both methods obtain rather regular segmentation with hardly any “salt and pepper” holes. The segmentation obtained by neural oscillators seems more delicate and closer to human perception: in the sagittal MRI (Magnetic Resonance Imaging), salient regions such as cortex, cerebellum and lateral ventricle are segregated with good accuracy; in the radar image, the cloud boundaries and eye of the hurricane are more precisely segregated.

6. CONCLUDING REMARKS

Inspired by neural synchronization mechanisms for perceptual grouping, simple networks of neural oscillators coupled with diffusive connections are proposed for visual grouping, and are compared to more standard methods such as graph cuts. The same general algorithm is shown to achieve promising results on several classical visual grouping problems, including point clustering, contour integration and image segmentation.

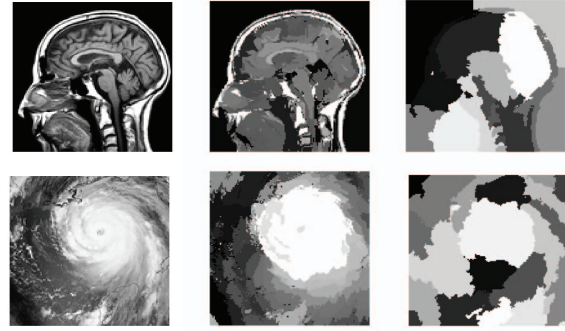


Fig. 9. Real image segmentation. From top to bottom, left to right: a sagittal MRI image (128×128); segmentation in 15 classes by neural oscillators and multiscale normalized cuts; a radar image (128×128); segmentation in 20 classes by neural oscillators and multiscale normalized cuts.

7. REFERENCES

- [1] G. Buzsaki. *Rhythms of the Brain*. Oxford University Press, USA, 2006.
- [2] K. Chen and D.L. Wang. A dynamically coupled neural oscillator network for image segmentation. *Neural Networks*, 15(3):423–439, 2002.
- [3] T.B. Cour, F. Benezit and J. Shi. Spectral Segmentation with Multiscale Graph Decomposition. *CVPR*, vol.2, 2005.
- [4] O. Faugeras, F. Grimberty, and J.J. Slotine. Stability and synchronization in neural fields. *S.I.A.M. Journal on Applied Mathematics*, 68(8), 2008.
- [5] D. J. Field, A. Hayes, and R. F. Hess. Contour integration by the human visual system: evidence for a local “association field”. *Vision Res*, 33(2):173-193, 1993.
- [6] R. FitzHugh. Impulses and physiological states in theoretical models of nerve membrane. *Biophysical Journal*, 1:445–466., 1961.
- [7] M. Kuzmina, E. Manykin, and I. Surina. Oscillatory network with self-organized dynamical connections for synchronization-based image segmentation. *BioSystems*, 76(1-3):43–53, 2004.
- [8] Z. Li. Computational Design and Nonlinear Dynamics of a Recurrent Network Model of the Primary Visual Cortex*. *Neural Computation*, 13(8):1749–1780, 2001.
- [9] W. Metzger. *Laws of seeing*. The MIT Press, 2006.
- [10] J. Nagumo, S. Arimoto, and S. Yoshizawa. An active pulse transmission line simulating nerve axon. *Proceedings of the IRE*, 50(10):2061–2070, Oct. 1962.
- [11] Q-C Pham and J-J Slotine. Stable concurrent synchronization in dynamic system networks. *Neural Netw.*, 20(1):62–77, 2007.
- [12] J. Shi and J. Malik. Normalized Cuts and Image Segmentation. *IEEE PAMI*, pp. 888-905, 2000.
- [13] W. Singer and C.M. Gray. Visual Feature Integration and the Temporal Correlation Hypothesis. *Annual Reviews in Neuroscience*, 18(1):555–586, 1995.
- [14] D.L. Wang. The time dimension for scene analysis. *Neural Networks, IEEE Transactions on*, 16(6):1401–1426, 2005.
- [15] W. Wang and J.J.E. Slotine. On partial contraction analysis for coupled nonlinear oscillators. *Biological Cybernetics*, 92(1):38–53, 2005.
- [16] R.J. Watt and W.A. Phillips. The function of dynamic grouping in vision. *Trends in Cognitive Sciences*, 4(12):447–454, 2000.
- [17] S.C. Yen and L.H. Finkel. Extraction of perceptually salient contours by striate cortical networks. *Vision Research*, 38(5):719–741, 1998.